DOI: 10.1002/ejic.201000147

A Bismuth-Stabilized Metal-Rich Telluride $Lu_9Bi_{\approx 1.0}Te_{\approx 1.0}$ – Synthesis and Characterization

Shalabh Gupta,[a] Paul A. Maggard,[b] and John D. Corbett*[a]

Keywords: Rare earths / Cluster compounds / Tellurium / Solid state chemistry / Hamilton populations

Synthetic reactions aimed at bismuth incorporation into rare-earth-metal-rich tellurides yielded $Lu_9Bi_{\approx 1.00}Te_{\approx 1.00}$ over a small range of compositions, but no analogues with Gd, Tb, Er, or Y. A single-crystal X-ray diffraction analysis gave the composition $Lu_9Bi_{0.99(3)}Te_{1.01}$ in the acentric orthorhombic space group $Cmc2_1$ at ambient temperature. This is isostructural with the re-refined Sc_9Te_2 earlier reported in a monoclinic *Cc* structure. $Lu_9Bi_{\approx 1.00}Te_{\approx 1.00}$ represents the first ternary compound in this structure type and the third lutetium-richest compound after Lu_8Te and Lu_7Te. The structure contains 3×3 columns of Lu in the form of condensed distorted *trans*-edge-sharing octahedral chains along *a*. The Te and Bi anions lie within tricapped trigonal prisms of Lu. Generally shorter Lu–Lu interactions lie in the interior of 3×3 metal columns compared with those on the periphery for which fewer Lu–Lu interactions and polar covalent bonding with neighboring tellurium weaken Lu–Lu bonding. Limiting Lu–Lu distances around 3.18 Å are by far the shortest among reduced lutetium tellurides. LMTO-type ab initio electronic structure calculations reveal a metallic nature and show that strong polar bonding of Lu to both the more electronegative Bi and Te leaves Lu relatively oxidized, many 5*d* states falling above the Fermi level. Stronger Lu–Lu bonding within the metal columns is also indicated by their larger individual Hamilton populations. The isostructural Lu_9SbTe and Sc_9BiTe were also shown to exist according to powder data.

Introduction

The quest for novel rare-earth (R) metal-rich condensed cluster phases and the understanding of their structural preferences and bonding characteristics have been challenging and rewarding endeavors in solid-state chemistry.[1,2] New structure types bearing unprecedented metal motifs in R-rich systems have improved our appreciation of structures, metal–metal bonding, ubiquitous packing effects, and of the importance of polar interactions therein for stability. Early examinations of such metallic systems with fairly electron-poor and delocalized bonding systems, incompletely filled bonding states (or a paucity of valence electrons), and metallic characteristics started with explorations of metal-rich cluster halides (X) of Zr and later were extended to those of group 3 (Y, Sc).[2,3] The incorporation of electron-richer late transition elements within the clusters has yielded unprecedented examples,[4,5] in part because of exceptionally strong hetero-metal bonding between early and late transition metal (*Tn*), as first inferred from Brewer's thermochemical studies[6] and more recently, from ab initio calculations.[7,8] For example, a considerable number of compounds in ternary mixed-metal systems (Y,Sc–*Tn*–X) have been since discovered in halide-poorer systems (R/X $\geq$ 1:1).[2] This chemistry has been successfully extended in more recent years to tellurides, resulting in an impressive collection of new structures, especially in ternary systems.[1,2,8,9]

One can easily envisage that, with twice the oxidation state of halide, only half as many mono-tellurium anions are required for charge neutrality with roughly the same oxidation states for R (ca. $+1 \pm 0.4$), thereby generating greater degrees of cluster condensation via metal–metal bonds.[1] In accordance, R-metal-rich tellurides exhibit many metal chains, 2-D sheets and 3-D networks, all of which feature isolated Te^{2-} anions centered in simple bi-or tri-capped trigonal prisms of R. The earlier known metal-rich group 4 transition-metal chalcogenides (Ti, Zr; S, Se)[10,11] and our discoveries of first rare-earth-metal examples Sc_2Te and $(Sc,Y)_8Te_3$[12,13] led us to examine other rare-earth metals. Intriguingly, only a few R-metals have been as productive as Sc and Y, the heavier Er and Lu, and a few examples with Gd, Dy and Ho.[9,14] Lutetium appears to be exceptional in this regard, including a few remarkable binaries such as Lu_7Te, Lu_8Te[15] with simple and elegant hexagonal packing of distorted Lu and Te layers, and $Lu_{11}Te_4$[16] with two independent condensed puckered Lu sheets separated by individual Te atoms, the metal sublattices being distinctively different from that in Sc_8Te_3 and the present structure. Y_7Te_2[17] is so far a curious binary

[a] Department of Chemistry, Iowa State University, Ames, Iowa 50011, USA
E-mail: jcorbett@iastate.edu
shalabh@iastate.edu
[b] Department of Chemistry, North Carolina State University, Raleigh, NC 27695, USA
E-mail: Paul_Maggard@ncsu.edu

Supporting information for this article is available on the WWW under http://dx.doi.org/10.1002/ejic.201000147.

example in which the structure is derived by formal replacement of Pd in $Y_6(Pd)Te_2$ (Sc_6PdTe_2-type) with Y to give $Y_6(Y)Te_2$.

We here report on our investigations in metal-rich phase space of the Lu–Bi–Te system, motivated by a general interest in the analogous pnictogen (Sb, Bi) systems. Particularly noteworthy are the absences of any Bi or Sb analogs of the binary R-rich tellurides; rather, the heavier R elements Gd–Lu only form one of the common structure types with 5:3 stoichiometries.[18,19] Only two R-metal-rich examples with mixed pnictogen-chalcogen anions have been reported, nonmetallic R_4Bi_2Te (R = Sm, Eu and Yb) with an *anti*-Th_3P_4 structure[20] and $Sc_6Bi_{1.68}Te_{0.80}$ with a Zr_6CoAs_2-type structure, an ordered ternary derivative of the Fe_2P type.[21]

Results and Discussion

Syntheses

Synthetic explorations in the Lu–Bi–Te system started with the detection of a new phase following a reaction with the composition Lu_6BiTe that was designed to explore pnictogen chemistry of R-metal-rich phases. Product distributions from reactions with nominal Lu/(Bi + Te) and Bi/Te proportions in the ranges of 4.5–2 and 2–0.75, respectively, suggest a fairly narrow phase width for the new Lu_9Bi_x-Te_{1-x} (as judged only by lattice dimensions; the precise ranges of x were not determined; see Table S1 in Supporting Information). Reactions with x = 0.5 and 1.5 resulted mainly in $LuBi_{1-y}Te_y$ (NaCl-type) and Lu for the former and an unidentified product for the latter. Extension to the analogous Ce, Gd, Tb, Er, and Y systems were not productive either in terms of the new orthorhombic phase or other new structures. A $Sc_9Bi_{\approx 1.0}Te_{\approx 1.0}$ phase with the new orthorhombic Lu_9BiTe structure was identified in ca. 60% yield with refined lattice parameters [a = 7.8151(4), b = 15.6600(8) and c = 17.3639(8) Å] that compare well with those of Sc_9Te_2[22] considering the sizes of Bi vs. Te. Further, the same new orthorhombic structure was also obtained in ca. 80% yield for the composition Lu_9SbTe, with a = 8.1319(8), b = 16.4854(8) and c = 18.2404(9) Å.

Structural Description

The near-[100] projection in Figure 1 shows the 3×3 atom nets of Lu that describe infinite columns of condensed clusters along a. The metal columns can be more clearly defined as the result of the side-by-side condensation of four chains of distorted edge-sharing octahedra in which adjoining chains are displaced by a/2, Figure 2. The former are in turn interlinked along b through an octahedral construction, giving rise to puckered metal sheets parallel to the ab plane. These sheets of metal columns are held together in the c direction by two independent Bi/Te anions, which at 100% occupancy refine to 72(1)% Te, 28% Bi at A1 and ≈ 73(1)% Bi, ≈ 27% Te at A2. Each of these is surrounded by nine Lu atoms in a tricapped trigonal prismatic (TCTP) arrangement (not marked). The trigonal prisms around both anion sites are fairly regular with an average A–Lu distance of 3.20 Å. The Lu–Lu prismatic edges around the predominantly Te (A1) and Bi (A2) sites range from 4.53–3.80 Å, [d(Lu–Lu)$_{avg}$ = 4.12 Å] around A1 and 4.57–4.08 Å, [d(Lu–Lu)$_{avg}$ = 4.15 Å] around A2, reflecting a somewhat larger major Bi site.

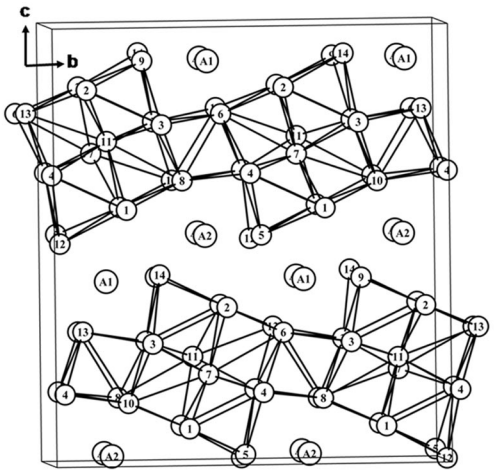

Figure 1. [100] representation of the unit cell of orthorhombic $Lu_9Bi_{0.99(3)}Te_{1.01}$. A1 and A2 are Te-rich and Bi-rich sites, respectively. Lu–Lu distances < 3.66 Å are outlined.

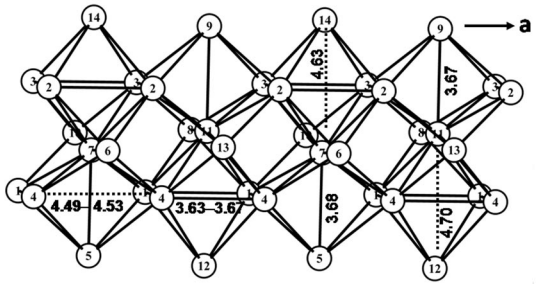

Figure 2. The edge-sharing and alternately distorted octahedra along the a axis in $Lu_9Bi_{\approx 1.0}Te_{\approx 1.0}$.

Structural contrasts of Sc_9Te_2 and, by implication, the present compound as well, with the electron-richer and higher symmetry Ti_9Se_2 have been described earlier.[22] Significant distortions of the fairly regular octahedral clusters that define Ti columns in Ti_9Se_2 (48 e^-) result from the lower electron counts for Sc_9Te_2 (39) and Lu_9BiTe (40), these leading to a fourfold increase in the cell size and a decrease in the symmetry from *Pbam* to *Cmc*2_1 (below).

The present discovery and refinement of $Lu_9Bi_{0.99(3)}$-$Te_{1.01}$ in the higher symmetry *Cmc*2_1 called for a reconsideration of essentially the same structure for Sc_9Te_2 in monoclinic *Cc*, which is a *translationengleiche* subgroup of *Cmc*2_1. Accordingly, the original reduced and corrected Sc_9Te_2 data set was re-refined in the orthorhombic cell starting with the present positions. This proceeded smoothly and uneventfully, and the two Te sites remained distinguishable. The new refinement for Sc_9Te_2 in C*mc*2_1 resulted in 10–18% lower residual parameters with two and

four fewer Te and Sc positions, respectively. No other significant structural changes were found. Positional correlations similar to those observed with $Lu_9Bi_{0.99(3)}Te_{1.01}$ persisted in both the high and low symmetry space groups. Crystal and refinement parameters for the re-refined Sc_9Te_2 are in Supporting Information.

Theoretical Considerations

Total and partial densities-of-states data from the electronic structure calculations on Lu_9BiTe according to the LMTO-ASA method[23] are shown in Figure 3 (top). Orbital components of the partial DOS data for Lu, Bi and Te are plotted in subsequent panels followed by the COHP analyses for all components. The compound's expected metallic nature is clear, with states around E_F heavily populated with Lu 5d and a little Lu 6p, a common feature of orbitally-rich and electron-poor compounds of the electropositive R.[7,8] The major Lu–Lu Hamilton populations in the COHP result[24] (black curve) come predominantly from 5*d*–5*d* interactions, with increasing mixing of 6*p* and 6*s* at lower energies. Not surprisingly, strong polar interactions result from overlap of Te 4p and Bi 5p orbitals with Lu orbitals over –6 to –3 eV for Te and –6 eV up to E_F for Bi. Although Lu–Bi bonding is fairly optimized, occupation of some Lu–Te antibonding states occurs just below E_F for the slightly more tightly bound Te. The dominant polar nature of the Lu interactions with Bi and Te and the effective oxidation of Lu that results are especially evident in the Lu PDOS data as well as in the total DOS. A large fraction of the Lu 5d states fall above E_F and are empty, which in effect leads to descreening of Lu 6s and 6p, their radial shrinkage and decreases in energy. Similar characteristics have been seen in recent studies of rare-earth-metal tellurides in other structures as well[7,8] and may be inferred from earlier extended Hückel results as well.[15,21]

The considerable numbers of independent distances between Lu atoms in this large and relatively low symmetry structure are difficult to sort out in detail. Extensive delocalization in the bonding is evident from the band results, so that reasons for all of the two-atom separations become quite opaque beyond some minimal matrix (size or packing) effects. We have evaluated pair-wise Hamilton populations for about 60 of the Lu–Lu "bonds" below 4.0 Å (d_{min} is 3.18 Å), and these clearly (and expectedly) show highly irregular relationships with the respective distances (Table S4). One obvious feature is that the individual Lu–Lu populations generally increase with the number of Lu neighbors. For example, the average population per "bond" for the six Lu that are more or less coplanar with Lu7 in the center of the upper column, Figure 1, is 0.52 eV/bond mol. In contrast, the average –ICOHP values for the six independent Lu–Lu "bonds" along the bottom edge of that sheet, between Lu4 and Lu1, average 0.34 eV. (The range in each set is still about 0.2 eV.) Similar but certainly not parallel orderings of Lu–Lu distances occurs elsewhere, but these are of course less meaningful than the Hamilton populations. And some fairly inexplicable –ICOHP magnitudes stand out too: Lu5–Lu7, Lu3–Lu3, and Lu9–Lu11, with distances over 3.65 Å, all have populations ≥ 0.45, showing how complex the bonding (and packing) can be.

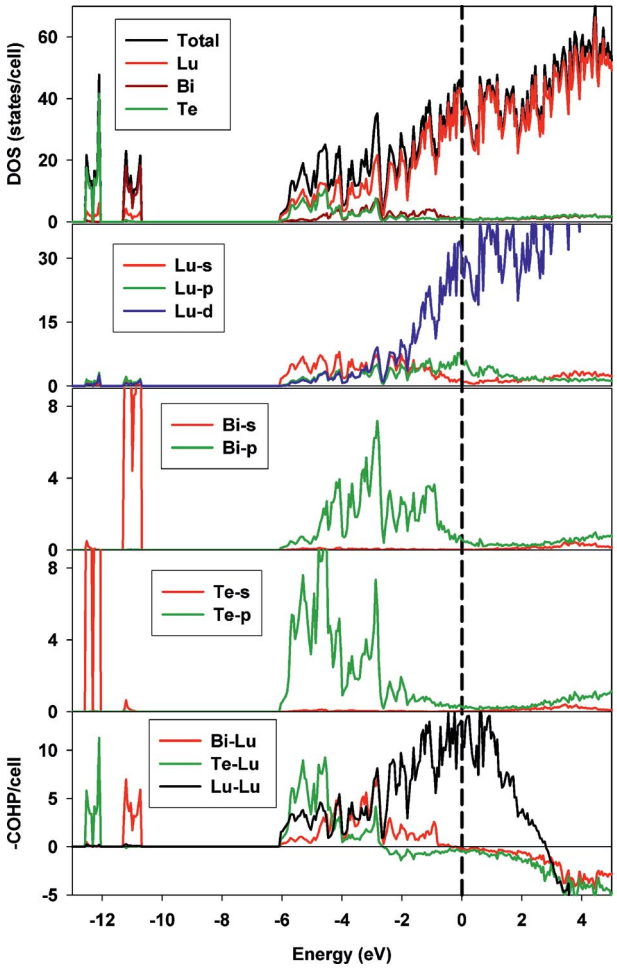

Figure 3. Densities-of-states (DOS), partial DOS by atom and orbital types, and the crystal orbital Hamilton populations (–COHP, eV per bond mol) for monoclinic (*Cc*) Lu_9TeBi. Pure Bi and Te in their predominant sites were input. The dashed line marks E_F.

Similar and appreciable variations among bond lengths according to their positions in rare-earth-metal frameworks have been noted before in the sheet structures of $Lu_{11}Te_4$ and Sc_9Te_2[16,22] as well as, more qualitatively, in many other tellurides. An irregular dependence of R–R distances on Mulliken overlap populations derived from earlier extended Hückel calculations were similar as far as the metal position in the extended array. This was at the time more specifically ascribed to the expectation that R–Te bonding (covalency) would raise the higher lying *d* states for the surface R atoms through mixing with the lower Te p states, an effect would be expected to weaken (and lengthen) the neighboring R–R bonds according to the number of Te neighbors. Although the R–Te bonding is probably a factor, this oversimplifies the R–R distance situation in complex intermetallic systems.

The creditability of ab initio LMTO-type calculations are sufficient that some useful ideas about the overall bonding

and stability in a diversity of novel phases can be derived in terms of the average –ICOHP sums for each bond type and their overall contributions in the entire structure. Such data for Lu_9BiTe are summarized in Table 1. The second column shows that the average –ICOHP value per bond for the polar Lu–Bi and Lu–Te contacts is at least twice as large as that for the average Lu–Lu interaction. However, the large multiplicity of Lu–Lu bonds in this fairly segregated structure, more than four times that for each of the polar types (column 3), overwhelms the larger effects for each Lu–Bi and Lu–Te contact in the total structure (column 4). Thus the Lu–Lu contributions comprise 52.0% of the total for the phase, the others making up about 24% each. The polar components clearly dominate in some other types of rare-earth-metal-rich phases with smaller R proportions in which, for example, condensed metal octahedra are propped open/centered by transition metal interstitials, e.g., $Er_7Au_2Te_2$, 50% Er–Au, and Pr_3RuCl_3, 56% Pr–Ru.[7,8]

Table 1. Individual (average) and cumulative –ICOHP components [eV] in Lu_9BiTe, $Z = 8$.

Atom pair	–ICOHP (avg., per bond; eV)	No. of bonds per cell	–ICOHP (cumulative, per cell; eV)	Contribution
Lu–Lu	0.344	84	28.9	52.0 %
Lu–Bi	0.745	18	13.4	24.1 %
Lu–Te	0.663	20	13.3	23.9 %

Conclusions

Synthesis of first pnictogen-stabilized R-rich telluride $Lu_9Bi_{\approx 1.0}Te_{\approx 1.0}$ has been achieved and with only a fairly narrow range of Bi/Te proportions. The isostructural Lu_9SbTe and Sc_9BiTe appear to exist as well. Analyses of ab initio electronic structure calculations by the COHP approach reveal that the polar bonding from Lu–Te and Lu–Bi contributions play a significant role in the bonding in the first, but that overall these are dominated by the more numerous Lu–Lu contacts in this very R-metal-rich phase. The relative oxidation of Lu by the electronegative Bi and Te is evident, with many of its 5d orbitals falling above E_F. Extensive electron delocalization appears to be characteristic of such a metal- and orbital-rich but electron-poor systems.

Experimental Section

Syntheses: All manipulations were carried out in nitrogen- or argon-filled glove boxes with less than 0.4 ppm H_2O levels. Ce, Gd, Er, Lu, Y, 99.95% total, Ames Laboratory; Sc turnings, 99.7% Aldrich-APL; Te ingots and Bi pieces 99.99%, Aldrich; Sb 99.9%, Johnson Matthey were used as received. Synthesis of the title phase started with Lu and BiTe which reduced Te and Bi volatilization during the initial arc-melting pre-reaction. Single phase BiTe (> 95%) was synthesized by heating a 1:1 molar ratio at 800 °C for 12 h. in a sealed evacuated silica container. Thereafter, pressed pellets of the appropriate mixtures were arc-melted under Ar at ≈ 25 amp current or less for 20 s on a water-cooled copper hearth within a glove box. The pellets were subsequently turned over and remelted to increase homogeneity. Weight losses during arc-melting reactions were a little over 1%. X-ray powder examinations revealed a new phase plus 10–15 vol.% of $LuBi_{1-x}Te_x$ (NaCl-type). Crushed samples were pelletized again, wrapped in molybdenum foil (to reduce possible Bi or Te attack on the inner Ta surface), sealed into tantalum tubes, and annealed between 1000 and 1200 °C for 1–2 weeks.

The first evidence of the title phase came from a nominal composition Lu_6Bi_2Te. Several subsequent reactions with varying Lu/(Bi + Te) and Bi/Te ratios (utilizing preformed LuBi and LuTe) revealed that the new phase formed for Lu/(Bi + Te) > 2 and Bi/Te ≥ 1 along with, principally, varying amounts of the mixed NaCl-type phase. Table S1 in Supporting Information lists several exploratory reactions, the products obtained, and the refined lattice constants of the new phase. These show only a small variations in the orthorhombic cell lengths and volumes (0.3–0.6%) were found, in parallel with the Bi/Te proportion, presumably following the ca. 0.14 Å larger single bond metallic radius for Bi.[25] X-ray diffraction-quality crystals were obtained after heating the nominal composition Lu_6BiTe at 1070 °C for 15 days. Yields as high as 90 (vol)% (+ ca. 10% NaCl-type) came from compositions ca. Lu_9BiTe. Adequate crystal growth could not be obtained for much higher or lower Bi/Te ratios. All attempts to synthesize the hypothetical limiting Lu_9Te_2 and Lu_9Bi_2 failed. Arc-melting the composition Lu_9Te_2 yielded mainly Lu_7Te[15] (along with some unidentified product), and these produced a mixture of Lu_8Te[15] and LuTe on annealing at 1100 °C. A Lu_9Bi_2 reaction at 1300 °C incorporated some Mo from the foil used to protect the pellet from the Ta and yielded Lu_6MoBi_2, a new congener of Lu_6MoSb_2[21] [Zr_6CoAs_2-type, $P\bar{6}2m$, a = 8.030(1) Å, c = 4.3052(9) Å] as identified from single crystal analysis.

Powder Diffraction: All products were analyzed by means of Guinier powder patterns secured from Huber 670 Guinier camera equipped with an image-plate and Cu-$K_{\alpha 1}$ radiation (λ = 1.540598 Å). Data were recorded at 293(2) K within the 2θ range of 4–100° over 30 min from samples held between two Mylar films with the aid of petroleum jelly and secured between the two Al rings of the sample holder. Product distributions on a volume basis were estimated from comparisons with powder patterns calculated from single crystal refinement data. Lattice constants of the new orthorhombic phase obtained from various synthetic compositions (Table S1) were calculated from least-squares refinement of measured and indexed reflections using the WinXPOW program.[26] The black compound is grossly stable for months to air at room temperature according to powder patterns of samples.

Semiquantitative EDS analyses of the single crystal used for X-ray diffraction and several others were performed with a JEOL 5910LV SEM equipped with a Noran–Vantage energy-dispersive spectrometer. The average composition from several spots on three different crystals was, normalized with respect to Lu, $Lu_9Bi_{0.84(4)}Te_{1.04(6)}$, in good agreement with the single crystal refinement result, $Lu_9Bi_{0.99(3)}Te_{1.01}$.

Structure Determination: Several irregular black crystals were checked for singularity and quality. Intensity data were collected with the aid of a Bruker APEX CCD-based X-ray diffractometer to $2\theta_{max}$ = 56.58° with 10 s/frame exposures. Intensity data were integrated and corrected for Lorentz, polarization and empirical absorption effects using the SAINT[27] and the SADABS[28] subprograms, respectively. A *C*-centered orthorhombic cell was indicated by the metrics of the data and the reflection condition $h + k = 2n$. Two possible space groups *Cmcm* and $Cmc2_1$ were indicated,

and the mean value of $|E^2 - 1| = 0.945$ favored the former centrosymmetric group. A total of 3103 unique reflections [$R_{int} = 7.8\%$] were used during the final refinement. A suitable starting model could not be obtained by direct methods however, suggesting an incorrect space group. A reasonable solution was then obtained in the non-centrosymmetric space group, $Cmc2_1$ and refined on F^2 with the aid of SHELXTL v6.10.[29] Of the twenty positions suggested by direct methods, four were discarded on the basis of distances and/or their irregular U_{iso} values after a few cycles of refinement, and the remainder were assigned as Lu. After a few more cycles the difference Fourier map was almost featureless and isotropic thermal parameters were all similar, which made assignment of the probable anion positions difficult. Nonetheless, two positions were assigned as Te and Bi according to the reported Sc_9Te_2 structure, which had equivalent lattice parameters but had been refined in the monoclinic space group, Cc ($Z = 8$) with 18 Sc and four anion positions.[22] The introduction of a mirror plane perpendicular to a and a screw axis along c also present in $Cmc2_1$ reduced the reported positions to 14 metal and two Bi/Te, and these led to the reported result. The provisional Bi and Te sites eventually refined as ca. 70:30 mixtures of Bi and Te. Some positional correlations between the anion sites and some metal positions could not be rectified by symmetry reduction to monoclinic Cc. No change in symmetry from $Cmc2_1$ was suggested by ADDSYM program in PLATON.[30] Anisotropic refinement at this stage led to elongated thermal ellipsoids with non-positive definite values for several Lu positions. This problem was well resolved by application of an improved, numerical absorption correction obtained with the aid of the X-Red[31] and X-shape[32] programs in the X-Area package, but without any gain with respect to the correlations. Semi-empirical absorption corrections with SADABS are often found inadequate for structures with large absorption coefficients (87.5 mm^{-1} here). The final anisotropic refinement (including twin corrections) converged at $R1 = 0.0514$, $wR2 = 0.1352$ for $I > 2\sigma(I)$. A refined Flack parameter of 0.47(4) supported the occurrence of racemic twins. We conclude that the largest residual electron densities, 3.89 (1.0 Å from Lu11) and –4.57 (0.68 Å from Lu12) e/$Å^3$ resulted from still imperfect absorption corrections as other parameters did not indicate any particular problems related to positional disorder. A high yield synthesis from the single crystal composition *per se* supports the correctness of the composition. Consistent results were obtained from two other crystals from same reaction. Some crystal and refinement parameters and the positional data with isotropic-equivalent displacement parameters are summarized in Tables 2 and 3, respectively. Positional coordinates have been reduced to the standard settings with STRUCTURE TIDY.[33]

Table 2. Selected crystal data and structure refinement parameters for $Lu_9Bi_{0.99(3)}Te_{1.01}$ and Sc_9Te_2.

	$Lu_9Bi_{0.99(3)}Te_{1.01}$	Sc_9Te_2
f.w.	1911.31	659.84
Crystal system	orthorhombic	orthorhombic
Space group, Z	$Cmc2_1$, 8	$Cmc2_1$, 8
Cell dim. /Å a	8.172(1)	7.7576(1)
b	16.550(3)	15.654(3)
c	18.300(4)	17.283(4)
Volume /$Å^3$	2475.0(9)	2098.8(7)
$\rho_{cal.}$ /g cm^{-3}	10.259	4.176
Data/res./param.	3120/1/118	2200/1/117
GoF on F^2	0.980	1.115
$R1$, $wR2$ [$I > 2\sigma(I)$]	0.0557/0.1287	0.0279, 0.0802
$R1$, $wR2$ (all data)	0.0665/0.1363	0.0294, 0.0812
Max., min. resid. /e $Å^{-3}$	3.89, –4.57	1.22, –1.26

Table 3. Atomic coordinates and isotropic equivalent displacement parameters ($Å^2 \times 10^3$) for $Lu_9Bi_{0.99(3)}Te_{1.01}$.

Atoms	Wyck.	Site sym.	x	y	z	U(eq)
A1[a]	8b	1	0.2454(2)	0.1195(1)	0.2759(2)	15(1)
A2[b]	8b	1	0.2514(2)	0.3710(2)	0.3775(2)	31(1)
Lu1	8b	1	0.2750(2)	0.1742(1)	0.4381(1)	24(1)
Lu2	8b	1	0.2751(2)	0.4257(1)	0.2131(1)	24(1)
Lu3	8b	1	0.2765(2)	0.2372(1)	0.1318(1)	25(1)
Lu4	8b	1	0.2775(2)	0.0138(1)	0.0189(1)	24(1)
Lu5	4a	m.	0	0.0232(2)	0.3738(1)	22(1)
Lu6	4a	m.	0	0.0761(2)	0.1512(1)	23(1)
Lu7	4a	m.	0	0.1141(2)	0.5577(2)	24(1)
Lu8	4a	m.	0	0.1755(1)	0.0000(1)	21(1)
Lu9	4a	m.	0	0.2741(1)	0.2742(1)	24(1)
Lu10	4a	m.	0	0.3174(2)	0.4941(1)	25(1)
Lu11	4a	m.	0	0.3658(2)	0.0918(2)	28(1)
Lu12	4a	m.	0	0.5136(1)	0.3595(1)	22(1)
Lu13	4a	m.	0	0.5693(2)	0.1581(1)	20(1)
Lu14	4a	m.	0	0.7649(2)	0.2857(2)	26(1)

[a] Bi1/Te1, 0.27(1)/0.73. [b] Bi2/Te2, 0.72(1)/0.28.

Band Calculations: Electronic densities-of-states for the title phase were calculated for the idealized (and practical) composition Lu_9Bi-iTe with the aid of the tight binding, linear-muffin-tin-orbital (TB-LMTO) method[34–36] within the atomic spheres approximation (ASA) with the Stuttgart code.[23] (The symmetry was reduced to Cc, with Bi and Te assigned according to their major populations.) Exchange and correlation were treated in the local density approximation,[37] and scalar relativistic effects were taken into account.[38] An automated procedure determined the radii of the Wigner–Seitz (WS) spheres, requiring that the overlapping potential be the best possible approximation to the full potential within the 16% limit for overlap between atom-centered spheres.[39] These fell in the ranges: Lu 1.709–1.849 Å; Bi 1.695 Å; and Te 1.685 Å. For space filling, 34 empty spheres (ES) with WS radii of 0.640–1.065 Å were also introduced within an 18% overlap limit with centered spheres. The basis set consisted of Lu-6s/(6p)/5d, Bi-6s/6p/(6d)/(5f), Te-5s/5p/(5d)/(4f) and a 1s/(2p) function for the empty spheres (down-folded[36,40] orbitals in parentheses); lutetium 4f orbitals were treated as filled core orbitals. The **k** space integrations were performed by the tetrahedron method[41] on grids of 554 irreducible k-points. For bonding analysis, the energy contributions of all filled electronic states for all Lu–Lu, Lu–Bi and Lu–Te atom pairs were calculated as a weighted function of the energy according to the crystal orbital Hamilton population (COHP) method.[24] Integration of COHP over all filled states gave ICOHP, the Hamilton overlap populations. The COHP data are plotted with reversed values with respect to energy (i.e., –COHP vs. E), as negative values correspond to bonding interactions.

Further details on the crystal structure investigation(s) for $Lu_9Bi_{0.99(3)}Te_{1.01}$ and for re-refined Sc_9Te_2 may be obtained from the Fachinformationszentrum Karlsruhe, 76344 Eggenstein-Leopoldshafen, Germany (Fax: +49-7247-808-666; E-mail: crysdata@fiz-karlsruhe.de), on quoting the depository numbers CSD-421463 and -421464.

Supporting Information (see also the footnote on the first page of this article): Supplementary material associated with this article [lattice constants from reactions with varying Lu/(Bi + Te) and Bi/Te ratios, detailed crystallographic, refinement, and displacement ellipsoid parameters, distances, and individual –ICOHP data].

Acknowledgments

We thank Ling Chen (Fujian Institute, Fuzhou, China) for the earliest investigations of the Lu–Bi–Te system. The guidance and insights of G. J. Miller are gratefully acknowledged. This research was supported by the National Science Foundation, Solid State Chemistry, via Grants DMR-0444657 and -0853732 and was performed in the Ames Laboratory of the U.S. Department of Energy.

[1] J. D. Corbett, in: *Inorganic Chemistry in Focus II* (Eds.: G. Meyer, D. Naumann, L. Wesemann), Wiley-VCH, Weinheim, Germany, **2005**, vol. 2, chapter 8.
[2] J. D. Corbett, *J. Alloys Compd.* **2006**, *418*, 1–20.
[3] A. Simon, H. Mattausch, G. J. Miller, W. Bauhofer, R. K. Kremer, in: *Handbook on the Physics and Chemistry of Rare Earths* (Eds.: K. A. Gschneidner, L. Eyring), Elsevier Science Publishers, Amsterdam, **1991**, vol. 15, p. 191.
[4] J. D. Corbett, *J. Alloys Compd.* **1995**, *229*, 10–23.
[5] J. D. Corbett, in: *Modern Perspectives in Inorganic Crystal Chemistry* (Ed.: E. Parthé), (NATO ASI), Kluwer Acad. Publ., **1992**, pp. 27–56.
[6] L. Brewer, P. R. Wengert, *Metallurg. Trans.* **1973**, *4*, 83.
[7] S. Gupta, K. Daub, G. Meyer, J. D. Corbett, planned publication.
[8] S. Gupta, J. D. Corbett, *Dalton Trans.*, manuscript in revision.
[9] N. Herzmann, S. Gupta, J. D. Corbett, *Z. Anorg. Allg. Chem.* **2009**, *635*, 848–854.
[10] J. P. Owens, H. F. Franzen, *Acta Crystallogr., Sect. B* **1974**, *30*, 427–430.
[11] a) T. E. Weirich, R. Poettgen, A. Simon, *Z. Anorg. Allg. Chem.* **1996**, *622*, 630–634; b) T. E. Weirich, R. Rmlau, A. Simon, S. Hovmöller, X. Zou, *Nature* **1996**, *382*, 144.
[12] P. A. Maggard, J. D. Corbett, *Angew. Chem. Int. Ed. Engl.* **1997**, *36*, 1974–1976.
[13] P. A. Maggard, J. D. Corbett, *Inorg. Chem.* **1998**, *37*, 814–820.
[14] P. S. Herle, J. D. Corbett, *Inorg. Chem.* **2001**, *40*, 1858–1864.
[15] L. Chen, J. D. Corbett, *J. Am. Chem. Soc.* **2003**, *125*, 7794–7795.
[16] L. Chen, S.-Q. Xia, J. D. Corbett, *Inorg. Chem.* **2005**, *44*, 3057–3062.
[17] L. M. Castro-Castro, L. Chen, J. D. Corbett, *J. Solid State Chem.* **2007**, *180*, 3172–3179.
[18] S. Gupta, E. A. León-Escamilla, F. Wang, G. J. Miller, J. D. Corbett, *Inorg. Chem.* **2009**, *48*, 4362–4371.
[19] A. Mar, in: *Handbook on the Physics and Chemistry of Rare Earths* (Eds: K. A. Gschneidner Jr., J.-C. G. Bünzli, V. K. Pecharsky), Elsevier Publishers, Amsterdam, **2006**, *36*, pp. 1–82.
[20] F. Hulliger, *Mater. Res. Bull.* **1979**, *14*, 259–262.
[21] L. Chen, J. D. Corbett, *Inorg. Chem.* **2004**, *43*, 436–442.
[22] P. A. Maggard, J. D. Corbett, *J. Am. Chem. Soc.* **2000**, *122*, 838–843.
[23] R. Tank, O. Jepsen, H. Burckhardt, O. K. Anderson, *Program TB-LMTO 47*, Max-Planck-Institut für Festkörperforschung, Stuttgart, Germany, **1994**.
[24] R. Dronskowski, P. E. Blöchl, *J. Phys. Chem.* **1993**, *97*, 8617–8624.
[25] L. Pauling, *Nature of the Chemical Bond*, 3rd ed., Cornell University Press, Ithaca, NY, **1960**, p. 403.
[26] *WinXPow 2.10*, Stoe & Cie GmbH, Darmstadt, Germany.
[27] *SAINT v6.22*, Bruker AXS. Inc., Madison, WI, **2000**.
[28] R. H. Blessing, *Acta Crystallogr., Sect. A* **1995**, *51*, 33–38.
[29] *SHELXTL 6.10*, Bruker AXS. Inc., Madison, WI, **2000**.
[30] A. L. Spek, *J. Appl. Crystallogr.* **2003**, *36*, 7–13.
[31] *X-RED 1.19*, STOE and Cie, Darmstadt, Germany, **1999**.
[32] *X-SHAPE 1.06*, STOE and Cie, Darmstadt, Germany, **1999**.
[33] L. M. Gelato, E. J. Parthé, *Appl. Crystallogr.* **1987**, *20*, 139–143.
[34] O. K. Andersen, *Phys. Rev. B* **1975**, *12*, 3060–3083.
[35] O. K. Anderson, O. Jepsen, *Phys. Rev. Lett.* **1984**, *53*, 2571–2574.
[36] W. R. L. Lambrecht, O. K. Anderson, *Phys. Rev. B* **1986**, *34*, 2439–2449.
[37] U. von Barth, L. Hedin, *J. Phys. C* **1972**, *5*, 1629–1642.
[38] D. D. Koelling, B. N. Harmon, *J. Phys. C* **1977**, *10*, 3107–3114.
[39] O. Jepsen, O. K. Anderson, *Z. Phys. B* **1995**, *97*, 35–47.
[40] P. Löwdin, *J. Chem. Phys.* **1951**, *19*, 1396–1401.
[41] P. E. Blöchl, O. Jepsen, O. K. Anderson, *Phys. Rev. B* **1994**, *49*, 16223–16233.

Received: February 6, 2010
Published Online: April 8, 2010

